

**FY92 PROGRESS REPORT FOR THE GYROTRON
BACKWARD-WAVE-OSCILLATOR EXPERIMENT**

T. A. Spencer
C. E. Davis
M. J. Arman
K. J. Hendricks

July 1993

DTIC
ELECTE
AUG 30 1993
S B D

Final Report

APPROVED FOR PUBLIC RELEASE; DISTRIBUTION IS UNLIMITED.

93 8 27 10 2

93-20216



PHILLIPS LABORATORY
Advanced Weapons and Survivability Directorate
AIR FORCE MATERIEL COMMAND
KIRTLAND AIR FORCE BASE, NM 87117-6008

This final report was prepared by the Phillips Laboratory, Kirtland Air Force Base, New Mexico, under Job Order 2301EP10. The Laboratory Project Officer-in-Charge was Dr. Thomas A. Spencer (WSR).

When Government drawings, specifications, or other data are used for any purpose other than in connection with a definitely Government-related procurement, the United States Government incurs no responsibility or any obligation whatsoever. The fact that the Government may have formulated or in any way supplied the said drawings, specifications, or other data, is not to be regarded by implication, or otherwise in any manner construed, as licensing the holder, or any other person or corporation; or as conveying any rights or permission to manufacture, use, or sell any patented invention that may in any way be related thereto.

This report has been authored by employees of the United States Government. Accordingly, the United States Government retains a nonexclusive royalty-free license to publish or reproduce the material contained herein, or allow others to do so, for the United States Government purposes.


This report has been reviewed by the Public Affairs Office and is releasable to the National Technical Information Service (NTIS). At NTIS, it will be available to the general public, including foreign nationals.

If your address has changed, if you wish to be removed from the mailing list, or if your organization no longer employs the addressee, please notify PL/WSR, Kirtland AFB, NM 87117-5776 to help maintain a current mailing list.

This report has been reviewed and is approved for publication.



THOMAS A. SPENCER, Ph.D.
Project Officer


CHARLES W. BEASON, Maj, USAF
Chief, Electromagnetic Source
Survivability Division

FOR THE COMMANDER


BRENDAN B. GODFREY, ST
Director, Advanced Weapons and
Survivability Directorate

DO NOT RETURN COPIES OF THIS REPORT UNLESS CONTRACTUAL OBLIGATIONS OR NOTICE ON A SPECIFIC DOCUMENT REQUIRES THAT IT BE RETURNED.

REPORT DOCUMENTATION PAGE			Form Approved OMB No. 0704-0188	
Public reporting burden for this collection of information is estimated to average 1 hour per response, including the time for reviewing instructions, searching existing data sources, gathering and maintaining the data needed, and completing and reviewing the collection of information. Send comments regarding this burden estimate or any other aspect of this collection of information, including suggestions for reducing this burden, to Washington Headquarters Services, Directorate for Information Operations and Reports, 1215 Jefferson Davis Highway, Suite 1204, Arlington, VA 22202-4302, and to the Office of Management and Budget, Paperwork Reduction Project (0704-0188), Washington, DC 20503.				
1. AGENCY USE ONLY (Leave blank)	2. REPORT DATE July 1993	3. REPORT TYPE AND DATES COVERED Final, Oct 91 - Sep 92		
4. TITLE AND SUBTITLE FY92 PROGRESS REPORT FOR THE GYROTRON BACKWARD-WAVE-OSCILLATOR EXPERIMENT		5. FUNDING NUMBERS PE: 61102F PR: 2301 TA: EP WU: 10		
6. AUTHOR(S) T. A. Spencer, C. E. Davis, M. J. Arman and K. J. Hendricks				
7. PERFORMING ORGANIZATION NAME(S) AND ADDRESS(ES) Phillips Laboratory 3550 Aberdeen Avenue SE Kirtland AFB, NM 87117-5776		8. PERFORMING ORGANIZATION REPORT NUMBER PL-TR--93-1011		
9. SPONSORING/MONITORING AGENCY NAME(S) AND ADDRESS(ES)		10. SPONSORING/MONITORING AGENCY REPORT NUMBER		
11. SUPPLEMENTARY NOTES				
12a. DISTRIBUTION/AVAILABILITY STATEMENT Approved for public release; distribution is unlimited.		12b. DISTRIBUTION CODE		
13. ABSTRACT (Maximum 200 words) Experimental and theoretical analyses, including particle-in-cell computer code simulations, are presented for the Gyrotron Backward Wave Oscillator (Gyro-BWO) high-power microwave device. The Gyro-BWO has been designed, constructed, and initially tested as a frequency tunable device. The design has concentrated on a TE ₀₁ , 4- to 6- GHz annular beam device. The annular beam is produced by the RAMBO pulser, which has a diode voltage of -300 to -800 kV and diode current of 1 to 20 kA. Initial results have shown that the device is operating in the backward wave mode. Initial results have also demonstrated that the device is magnetically tunable; that is, the frequency is tunable by adjusting the magnetic field. A Vlasov-type antenna is used for the extraction of the microwave signal on the diode end of the experiment, with initial power extraction of up to 2 MW.				
14. SUBJECT TERMS High Power Microwave, HPM, Gyro-BWO, Gyrotron Gyrotron Backward Wave Oscillator			15. NUMBER OF PAGES 50	
			16. PRICE CODE	
17. SECURITY CLASSIFICATION OF REPORT Unclassified	18. SECURITY CLASSIFICATION OF THIS PAGE Unclassified	19. SECURITY CLASSIFICATION OF ABSTRACT Unclassified	20. LIMITATION OF ABSTRACT SAR	

PREFACE

This progress report is based on experimental and theoretical work performed on the Gyrotron Backward Wave Oscillator conducted in FY92 at the Phillips Laboratory. The authors would like to acknowledge the following people for their help and support of the Gyro-BWO experiment: Walter Fayne, Ralph Perado, and Melody Kipp (Air Force Phillips Laboratory); Dr. Ronald Gilgenbach (University of Michigan); Rudy Sedillo, Mike Scott, and Dale Ralph (Maxwell Labs). This experiment is funded in part by the Air Force Office of Scientific Research (AFOSR).

DTIC QUALITY INSPECTED 3

Accession For	
NTIS GRA&I	<input checked="checked" type="checkbox"/>
DTIC TAB	<input type="checkbox"/>
Unannounced	<input type="checkbox"/>
Justification	
By	
Distribution/	
Availability Codes	
Dist	Avail and/or Special
A-1	

CONTENTS

<u>Section</u>		<u>Page</u>
1.0	INTRODUCTION AND BACKGROUND	1
2.0	ANALYSIS, SIMULATIONS AND DESIGN	2
3.0	EXPERIMENTAL RESULTS	13
4.0	CONCLUSIONS AND FUTURE WORK	16
	REFERENCES	17
	APPENDICES	
	A. RADIATION HAZARD CALCULATIONS	18
	B. SAMPLE CRYSTAL DIODE CALIBRATION	20
	C. SAMPLE CABLE CALIBRATION	23
	D. ASYST CHANNEL SETUPS	26
	E. SAMPLE MAGNET INPUT DATA DECK FOR THE GYRO-BWO	32
	F. SAMPLE EGUN INPUT DATA DECK FOR THE GYRO-BWO	37

1.0 INTRODUCTION AND BACKGROUND

The Gyrotron Backward-Wave-Oscillator (Gyro-BWO) is a device that is new to the Air Force Phillips Laboratory. The device has been designed, constructed, and tested in FY92. The device works on the electron cyclotron instability (the so-called 'negative mass' instability) and is a frequency tunable device. The frequency is tuned by means of adjusting the interaction region magnetic field (to be discussed later). Intramode tuning is possible by small adjustments to the magnetic field, and inter-mode tuning is possible by larger adjustments to the magnetic field. The device excites a backward wave (a wave that propagates antiparallel to the e-beam) based on the electron beam (e-beam) and interaction region parameters. Based on these parameters, the backward wave frequency is given by the intersection of the cylindrical waveguide (interaction region) dispersion lines and the e-beam dispersion line. Distinct advantages of the device over conventional BWOs is the simplicity of the interaction region. The interaction region is a smooth cylindrical tube. Conventional BWOs use a periodic structure (either sinusoidal or perhaps a polynomial variation) which can reduce the powerhandling capabilities of the device, and are usually more difficult to construct. Gyro-BWOs have another advantage in that they tend to be less sensitive to e-beam velocity spreads than other standard devices (such as the Gyrotron and especially the Cyclotron AutoResonance Maser [CARM]). This is advantageous when using a cold-cathode (field emission cathode) diode configuration, since cold-cathodes tend to have poor quality e-beams. For most high-power microwave work, the system requires a high-power e-beam to extract high-power RF. Cold-cathode technology is presently the method a high power e-beam is generated.

The design of the Gyro-BWO is based on previous work done by S. Y. Park, *et. al.* (Ref. 1) and T. A. Spencer, *et. al.*, (Refs. 2 and 3). Early experimental work involved small currents (<10 A) and low voltages (<100 kV) (Refs. 1, 4, and 5) which produced relatively low powers (~ 10 kW) but reasonable efficiencies of ~ 15 percent. The work conducted in References 2 and 3 consisted of high-current (250 to 1500 A), high-voltage (500 to 700 kV) Gyro-BWO experiments, with both an annular e-beam (max of about 300 A) and solid e-beam (maximum of about 1500 A). Reasonable power was obtained (~ 8 MW), but at poor efficiencies (1 to 2%). Theoretical analysis of the Gyro-BWO exists in References 6-8.

2.0 ANALYSIS, SIMULATIONS AND DESIGN

A basic analysis of the device can be done based on the decoupled dispersion relation between the interaction cavity (cylindrical waveguide) and the e-beam. The equation for the vacuum waveguide dispersion relation is

$$\omega^2 - k_c^2 c^2 - k_z^2 c^2 = 0$$

where c is the speed of light, k_c is the cutoff wavevector for a cylindrical waveguide, and k_z is the axial wavevector. The equation for the doppler-shifted e-beam dispersion relation is

$$\omega - k_z v_z - s\Omega_r = 0$$

where v_z is the axial velocity, s is the harmonic number ($s = 1$ being the fundamental), and Ω_r is the electron relativistic cyclotron frequency given by

$$\Omega_r = \frac{eB}{\gamma m}$$

where e is the elementary charge, B is the magnetic field, γ is the Lorentz relativistic factor, and m is the mass of the electron. The vacuum waveguide and e-beam dispersion equations are then solved simultaneously to provide the frequency and wavenumber information.

The work done in References 2 and 3 consisted of a TE₁₁ (azimuthal variation = 1, radial = 1) mode experiment in the frequency range of 4.5 to 6 GHz. The radius of the interaction region was 1.93 cm, which is rather small and can breakdown at high RF power. The present interest is to have a frequency range of 4 to 6 GHz, but with a larger radius to handle a larger amount of power. Thus it was decided to try to operate in the TE₀₁ mode, which, for a frequency cutoff of ~4.2 GHz, gives a radius of ~4.37 cm (See Ref. 2 for the equations to solve for the radius, etc.). The interaction cavity length is 15 cm (based on the magnetic field configuration, to be discussed, and recent experiments done at the University of Michigan Ref. 9). Based on the choice of radius and mode operation, the dispersion equations were solved to obtain a magnetic field range to operate at the desired frequency. An example of the dispersion curve with corresponding parameters is shown in Figure 1. The parameters are: $\alpha = v_\perp/v_\parallel = 0.5$, Energy = 390 kV, Radius = 4.37 cm, B-field = 3.2 kG, Current = 1000 A. The backward wave

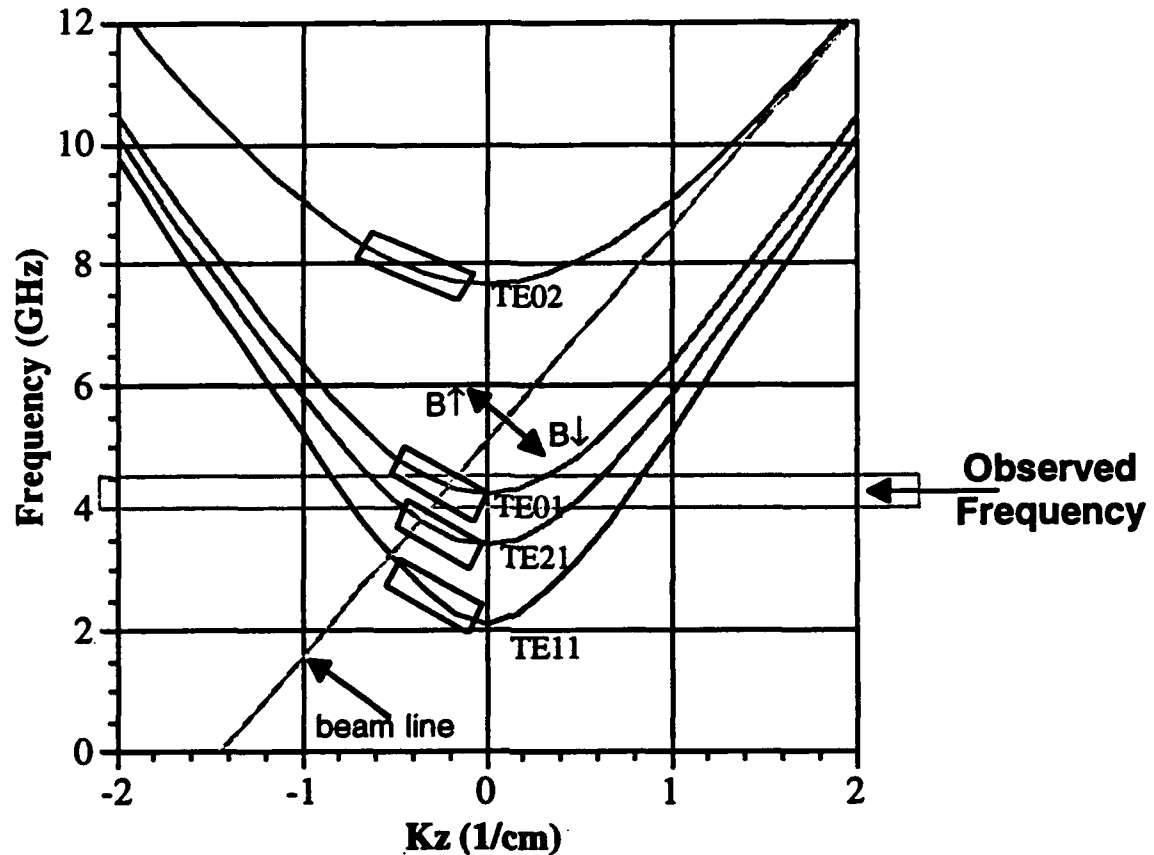


Figure 1. Typical dispersion curve showing the various backward wave intersections.

frequency intersections are: $TE_{11} = 3.25$ GHz, $TE_{21} = 3.81$ GHz, $TE_{01} = 4.35$ GHz, $TE_{02} =$ None. The observed frequency is that which is being concentrated on in the actual experiments (to be discussed later). The small rectangular boxes are the approximate operating frequencies for the given mode. Mode competition is a problem and will have to be addressed in future experiments.

The original design of the experiment was to use the IMP pulser to provide the e-beam, but due to the availability of the RAMBO pulser (and other experiments being conducted using IMP), it was decided to utilize the RAMBO pulser for the experiment. Only minor design alterations were necessary since the pulsers are similar in voltage and current output. The RAMBO e-beam parameters are voltage = -400 to -800 kV; diode current 1 to 40 kA; and pulse length = 0.3 to 3 μ s. The actual current that reaches the interaction region (called the tube current) varied from 250 to 1000 A, depending on the magnetic field configuration. Due to the large voltage and current parameters to be used in the experiment, a radiation hazard calculation was necessary.

Appendix A shows the amount of x-rays produced at the maximum operating parameters of the experiment.

The actual experimental configuration is shown in Figure 2. The e-beam is generated from an immersed field cathode (of which the diode field can be varied up to 1.5 kG), travels through the drift tube towards the interaction region where it is adiabatically compressed by the maser magnetic field coils (which can be varied from 3 to 7 kG). The maser magnetic field coils are used to tune the frequency. The e-beam then interacts with the cavity modes, producing a backward wave (if the given parameters are correct). The e-beam leaves the interaction region and is dumped into the drift tube wall by a pair of horse-shoe shaped, 500 G magnets.

The backward wave that is produced in the interaction cavity propagates back towards the diode region where it is partially extracted by a Vlasov-type C-Band (frequency cutoff of 3.16 GHz, TE_{10} [rectangular mode] matched in the frequency range of 3.95 to 5.85 GHz). A calibration to determine the efficiency of the antenna has yet to be done (that is, the ratio of the RF power extracted into the waveguide by the antenna to the RF power actually produced in the drift tube). The nonextracted backward wave continues into the diode region where it eventually dissipates, or in the case of a stainless steel anode screen (or carbon anode screen), the backward wave is absorbed or reflected back towards the downstream end of the experiment. A C-Band standard gain horn is placed on axis ~170 cm from the output window to measure any RF signal (note that this is not the optimum position for the TE_{01} mode pattern, but is set up to measure any TE_{11} signal that may exist).

After being partially extracted by the antenna, the RF signal travels through a series of waveguide directional couplers, low-pass, band-pass, and high-pass filters, and is detected by crystal diode detectors. Sample calibration setups for the crystal diodes and the cables are shown in Appendices B and C. The waveguide and Vlasov-type antenna are separated by a 0.64 cm lucite window (to break the machine [RAMBO pulser] ground from the ground of the waveguide; it also provides a vacuum seal). Figures 3, 4, and 5 show the waveguide RF detector setup. (Note that the heterodyne signal from the Wavetek Micro Source [model 954] shown in Figure 4 was not initially employed and is to be used in the FY93 experiments). The signals are then displayed on various oscilloscopes and the data is transferred to a computer via the ASYST software package. The scope channel setups used in ASYST are given in Appendix D.

Several computer codes were used to assist in the design and analysis of the Gyro-BWO experiment. Magnet, a steady state computer code written by John Freeman (Sandia National

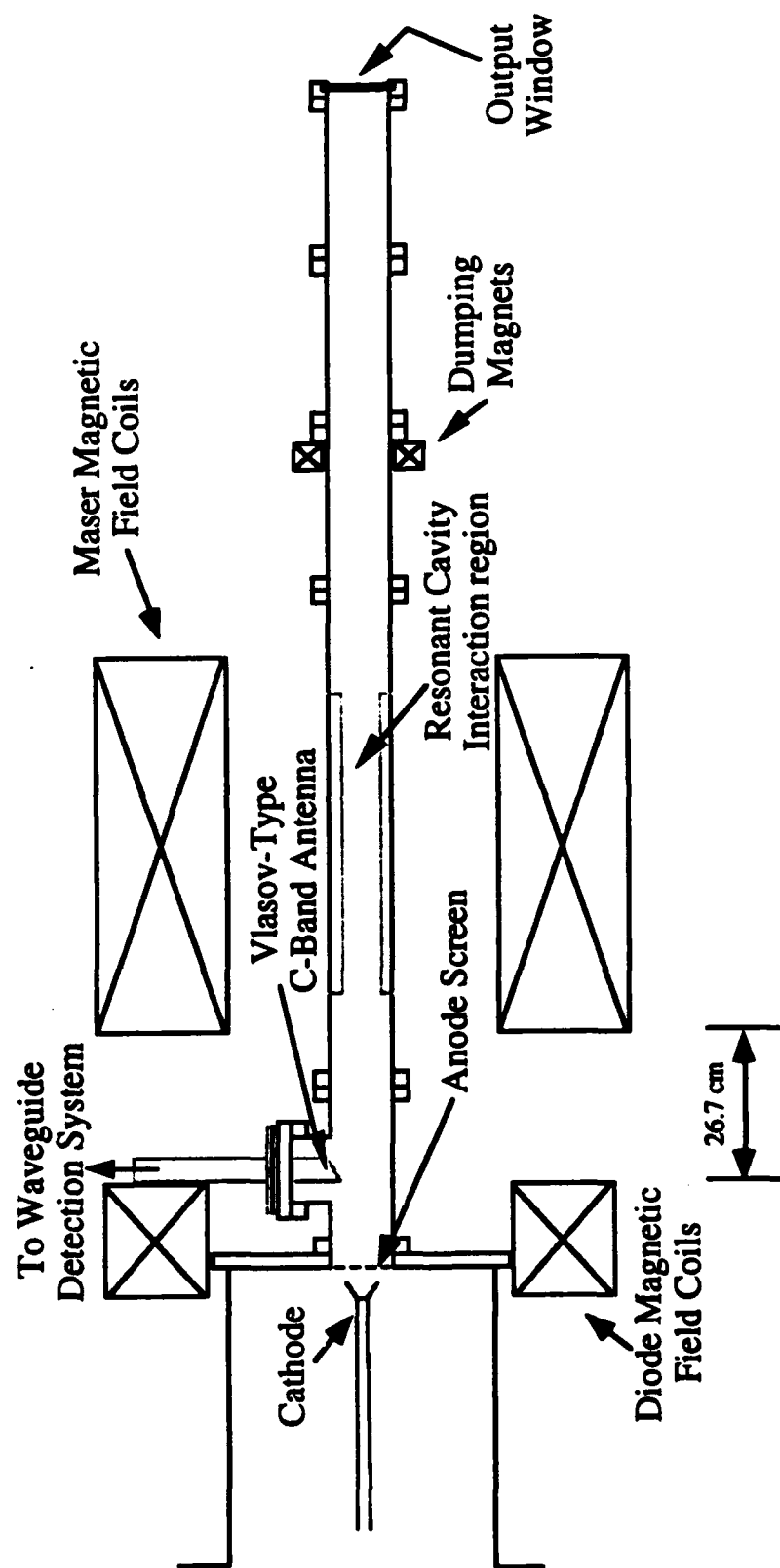


Figure 2. The Gyro-BWO experimental configuration.

C-Band: $F_{co} = 3.16$ GHz
TE₁₀ matched -> 3.95 - 5.85 GHz

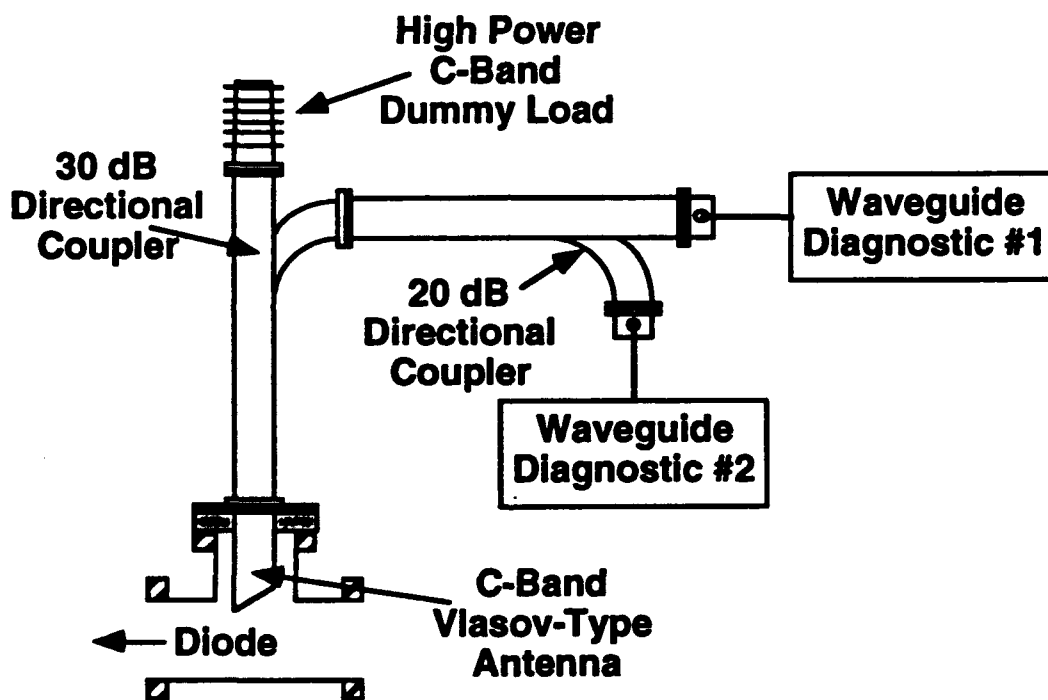


Figure 3. Waveguide components connected to the C-Band antenna used to detect the backward wave RF signal.

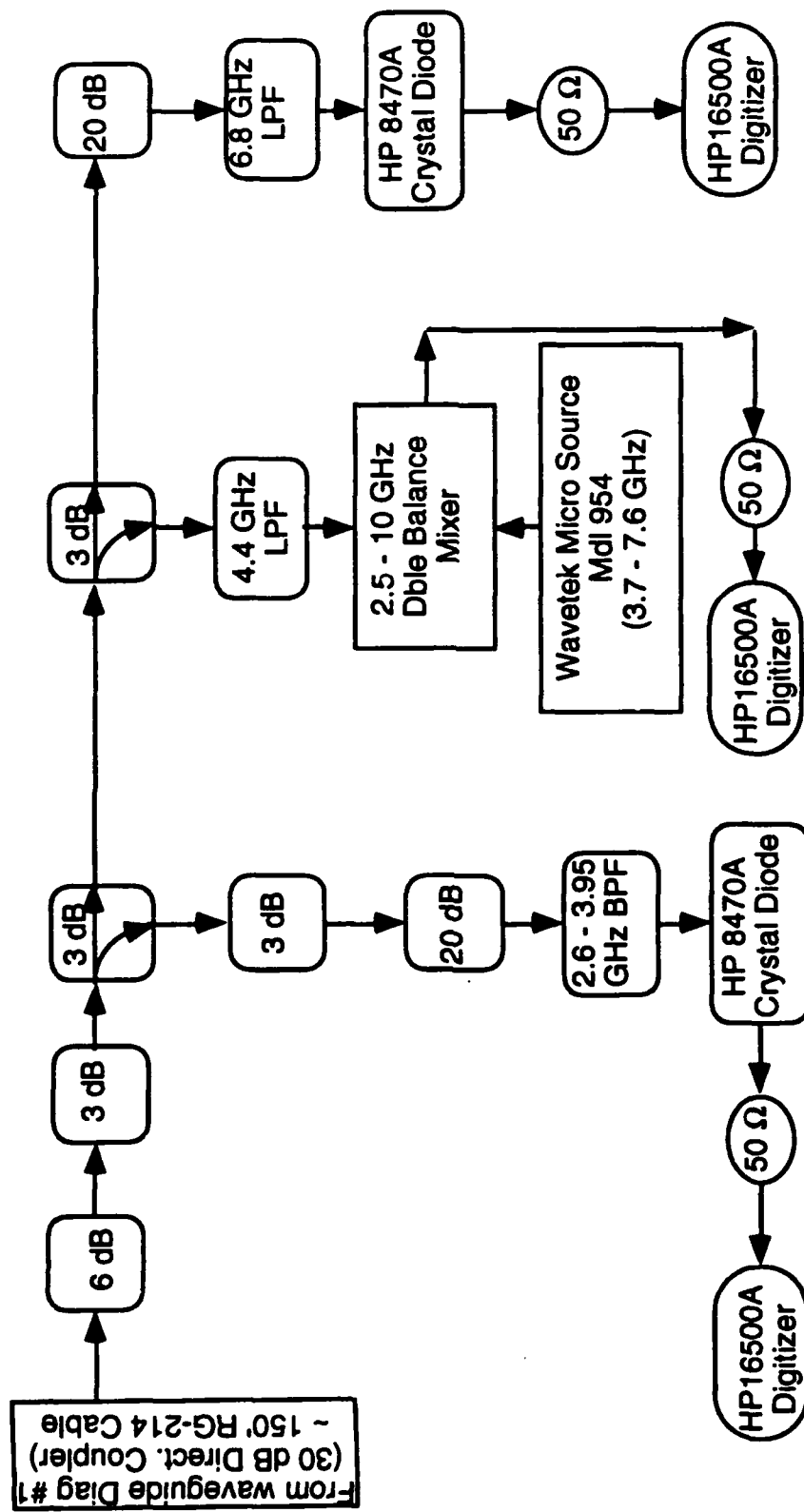


Figure 4. Attenuators, filters and crystal diode detector setups for Waveguide Diag #1 (Fig. 3).

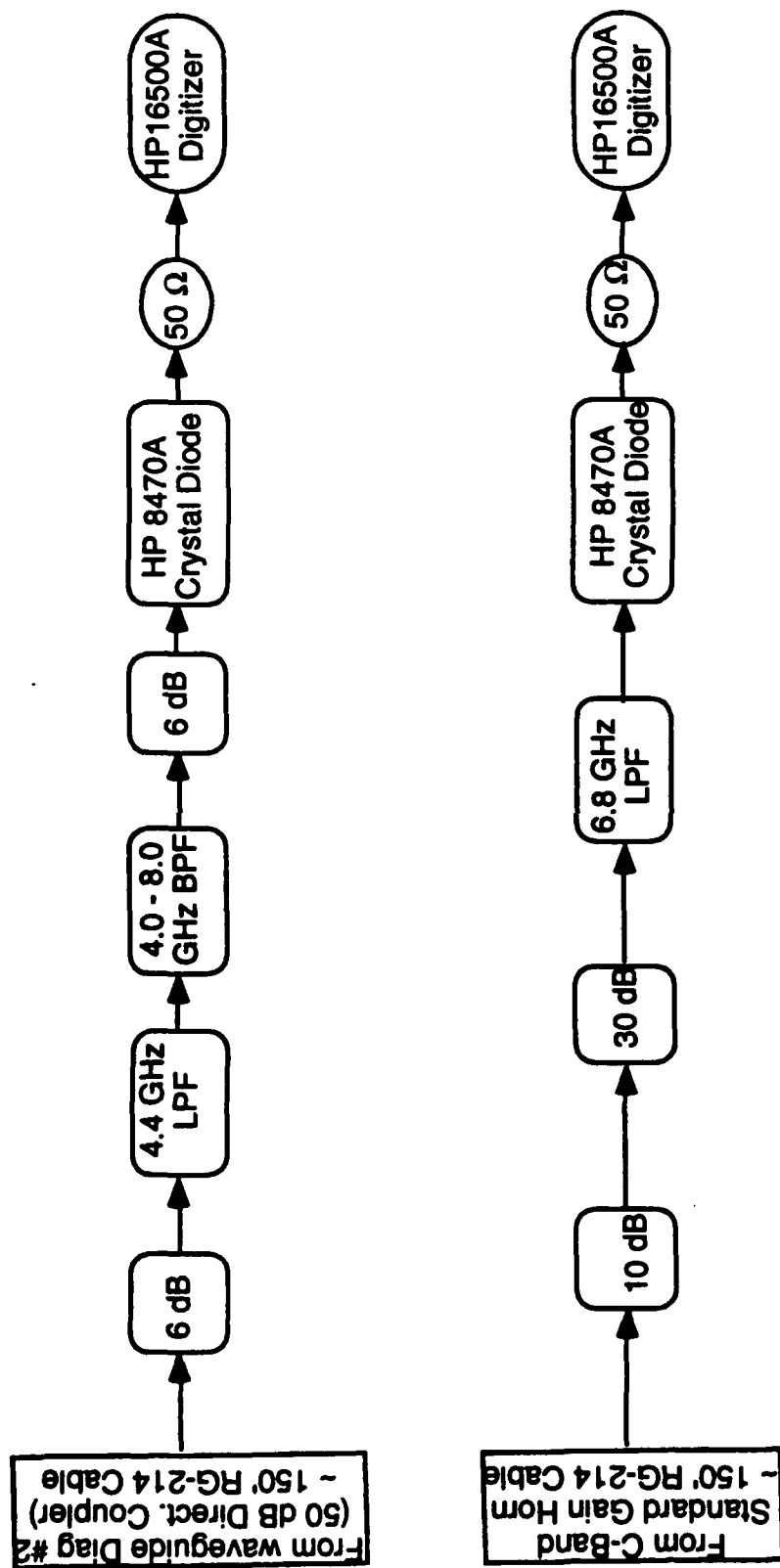


Figure 5. Attenuators, filters, and crystal diode detector setups for Waveguide Diag #2 (Fig. 3), and the C-Band standard gain horn (located downstream, on-axis, ~170 cm from the lucite output window (Fig. 2)).

Laboratories-Albuquerque [SNLA], with corrections and updating by Bill Tucker, SNLA, on 9/24/85 for a PC; converted for a Macintosh by Thomas Spencer, 6/12/92) was utilized to find the optimum configuration for the DC magnetic field coils (located over the diode region) and the Helmholtz magnets. An example of an input file is included in Appendix E. Note that at this point only the center set of the DC coils are used (there are three sets of coils connected together). Figure 6 has an example of the Helmholtz setup (current of 1020 A) with the DC Coils (current of 300 A) predicted from Magnet, with a fairly uniform distance of ~15 cm in the Helmholtz region. The cathode location in Figure 2 is located at 39 cm in Figure 6 (corresponding to an AK gap of 2.5 cm). The DC Coil is located ~26.7 cm away from the first magnet of the Helmholtz pair magnets. Figure 7 has the actual measured value obtained with a fast Hall Effect probe and also shows a fairly uniform field over ~15 cm. Based on this length of magnetic field and recent results from the University of Michigan showing a cavity length of ~15 to 17 cm produced similar output powers as a 50 cm length (Ref. 9), a cavity length of 15 cm was chosen.

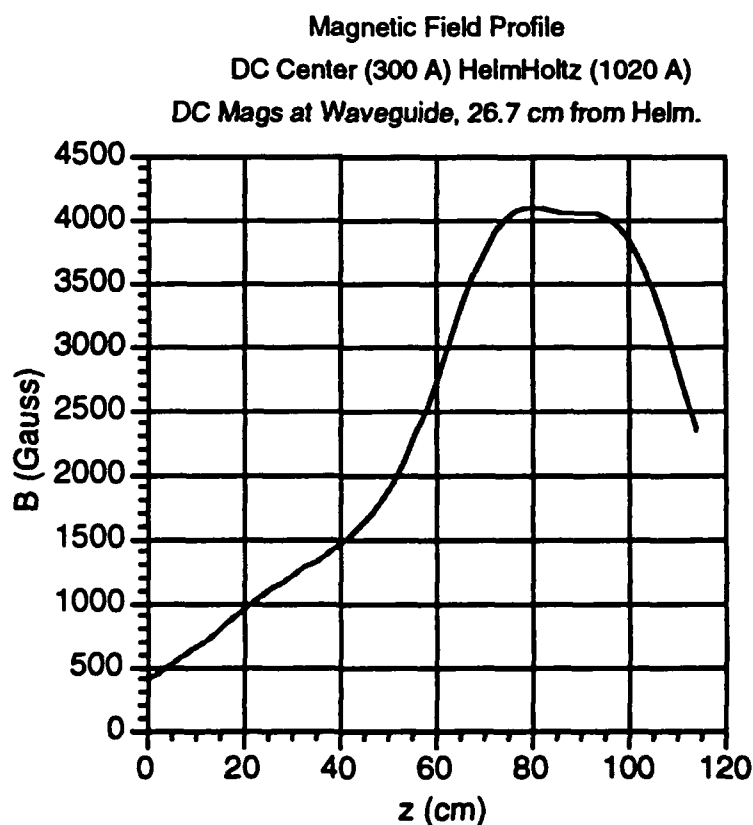


Figure 6. Theoretical DC Coil and Helmholtz Coil curve obtained using the computer code Magnet.

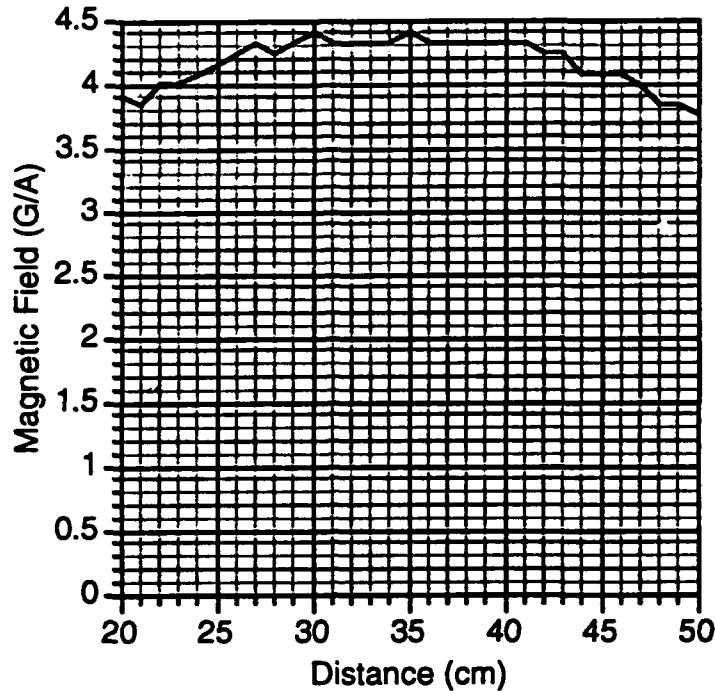


Figure 7. Measured Helmholtz coils curve obtained using a fast Hall Effect probe. Only the center region of the Helmholtz coils is shown (zero corresponds to the outer edge of the first coil of the Helmholtz pair; zero also corresponds to the diode end of the experiment).

Another computer code used was the EGUN code (Ref. 10), which is an electron trajectory code used for diode design. A spatially varying magnetic field was input based on the measured magnetic fields (a short computer program was written to superimpose the two magnetic fields; DC and Helmholtz). An example of an EGUN input data file is included in Appendix F. An annular cathode was designed, with the outer radius chosen in such a way that when the beam traversed the compression portion of the magnetic field, the beam would be focused to ~ 1.95 cm (outer radius). This was done since the TE_{01} peak E-field location is located at this radial position in the interaction cavity (which can be found by looking at the peak of the Bessel function in the r direction). The effect is to increase the coupling between the RF wave of the TE_{01} mode and the e-beam. From the results of the code runs, it was decided to place a stainless steel anode screen into the experiment to allow for more current to propagate down the drift tube. Figure 8 shows an example of the original diode design (see the figure for parameters). After the anode screen was placed in the experiment, the screen ceased to exist after only a few shots, and it was decided to do away with the screen. This caused a fair amount of the e-beam (up to 90 percent) to be lost by scraping on the drift tube wall, but it also allowed for a higher α (v_{\perp}/v_{\parallel}), which is necessary for a high efficiency Gyro-BWO device. This also shortens the beam pulse and creates a triangular voltage pulse (thus limiting the RF pulse; see Section 4.0) rather than a

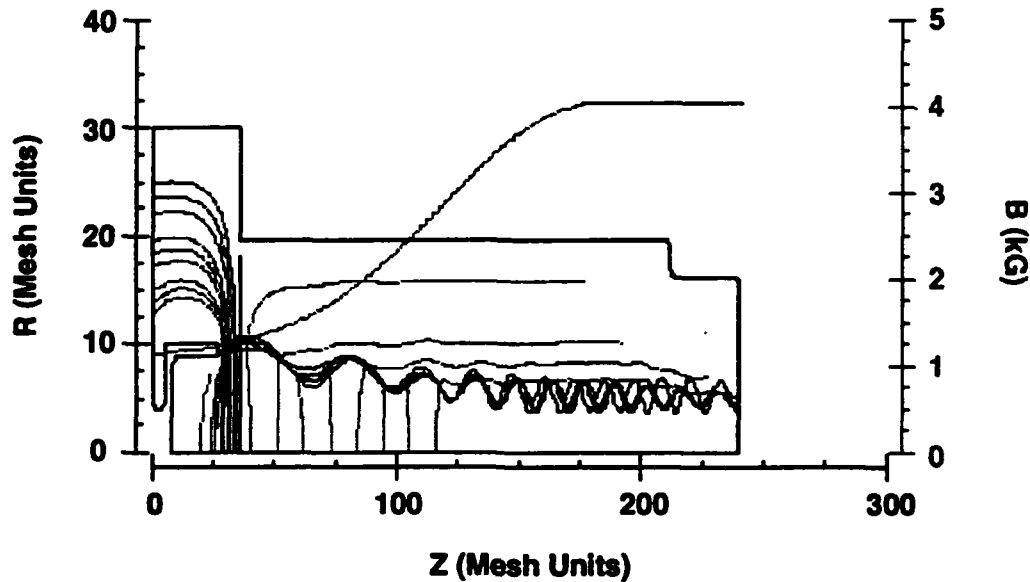


Figure 8. EGUN simulation showing the electron trajectories, the equipotential lines, and the magnetic field for a 550-kV e-beam and a gap of ~ 2.5 cm (0.25 cm/mesh). (Note that this was one of the original designs, which contained a thin anode screen mesh.)

flat-top voltage pulse. Part of the FY93 work will be to increase the RF pulse by reconfiguring the diode. Again, EGUN (and also MAGIC) will be used for the updated diode design.

MAGIC (Ref. 11) is another computer code (a 2 1/2-D Particle-In-Cell [PIC] code) used for analysis and design of the Gyro-BWO. Many hours were spent getting the code to simulate the Gyro-BWO. Initial runs had boundary condition problems, in particular the exit boundary in trying to make the beam 'go-away'. It is now felt that an adequate solution to the exit boundary problem has been ascertained. The present simulations appear to imply a growing TE_{02} forward gyrotron interaction is the dominant interaction (as demonstrated in Figure 9, with the main frequency at about 10 GHz), which is not what was expected. Figure 9 shows the results of a MAGIC simulation for parameters of Voltage = 550 kV; Current = 5 kA; Magnetic Field = 4 kG; Radius (cavity) = 4.37 cm; Alpha = 0.5. Both figures are the E_θ component located at the output end of the simulation. The left figure in Figure 9 is the time history of the exit boundary E_θ component of the RF wave which shows that the RF wave saturates. The right figure in Figure 9 shows the frequency spectrum of the left figure in Figure 9, showing the 10 GHz frequency is dominant.

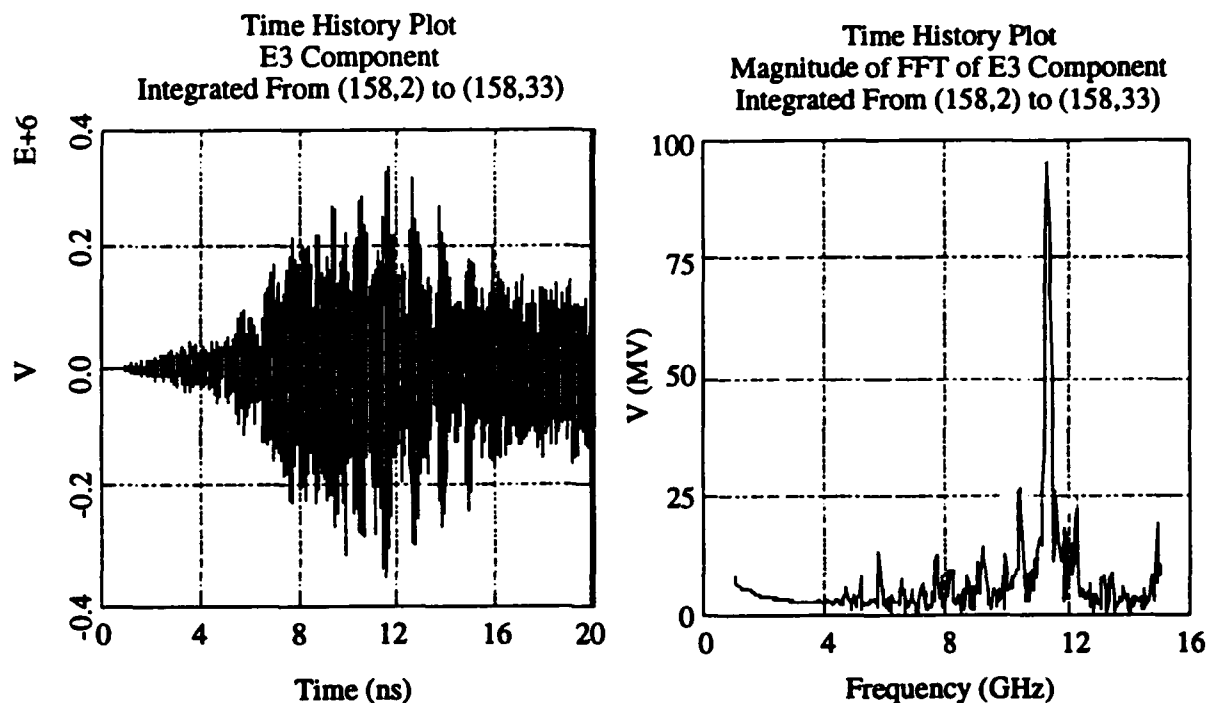


Figure 9. MAGIC simulation results.

Expected dominate frequency was around 4 to 5 GHz (TE_{01} mode). Diagnostics placed at the entrance end of the tube in the simulation show similar results (not shown). The belief that this is a TE_{02} forward gyrotron interaction is deduced from the dispersion curve in Figure 1. One possible reason for the TE_{02} mode being dominant may be the amount of current (5 kA) used in the simulation. Simulations are continuing to investigate this possibility. At present, the experimental diagnostics have not been set up to observe any RF in the 9- to 12-GHz range. This will be done in the future.

3.0 EXPERIMENTAL RESULTS

The experiment was constructed and configured for operation late in FY92. The first shots on the machine were taken in early September. This did not allow for ample data taken in FY92. The initial results were encouraging and demonstrated that the device is working correctly, although the device is far from optimized. Initial results concentrated on the frequency range of 4.0 to 4.4 GHz. Figures 10 and 11 show some typical data obtained from the initial experiments. The diode magnetic field for Figures 10 and 11 was ~ 500 G and the interaction magnetic field was ~ 4.3 kG. Figure 10 has a Marx voltage trace, a current trace of the current inside the cavity interaction region, and an extracted microwave signal. Notice that the voltage pulse is triangular, which is due to diode closure effects. The optimum voltage pulse would have at least a 500- to 600-ns flat-top. Also note that the current is only 250 to 300 A, approximately 10 to 15 percent of the measured cathode shank current (not shown) of ~ 2200 A. This implies much of the current is lost somewhere in the experiment, probably colliding into the drift tube wall. Inspection of the drift tube section proved that the beam was colliding with the wall, and this was probably causing the triangular voltage pulse. An improved diode configuration will be tested at a later date.

The data shown in Figure 11 demonstrate that most of the detected RF signal lies within the frequency range of 4.0 to 4.4 GHz. The upper left plot in Figure 11 shows the detected signal in the frequency range of 2.6 to 3.95 GHz (it has an effective lower range cutoff of 3.2 GHz, since this is the cutoff of the C-Band waveguide, but the band-pass filter used actually had a frequency range of 2.6 to 3.95 GHz). The lower left plot in Figure 11 shows the detected signal in the frequency range of 4.0 to 4.4 GHz. The lower right plot in Figure 11 shows the detected signal in the frequency range of 3.2 to 6.8 GHz.

Initial frequency tunability was also demonstrated by varying the magnetic field and observing the detected RF signals in the given band-pass filter diagnostics. As the magnetic field was increased above the 4.3 kG used for the data obtained in Figures 10 and 11, the detected RF signal in the 4.0 to 4.4 GHz band-pass filter decreased and eventually disappeared, whereas the detected RF signal in the 3.2 to 6.8 GHz band-pass remained, albeit at a lesser power.

Essentially no signal was seen in the 2.6 to 3.95 GHz band-pass filter. This result demonstrated two things: (1) The RF signal is magnetically tunable and (2) the device is truly operating as a Gyro-BWO. The second result can be deduced from the dispersion curve plot shown in Figure 1. As the magnetic field is increased, the intersection between the waveguide mode and the e-beam also increases (on the backward wave side; that is, $k_z < 0$). Note that this is not true in the case of a gyrotron forward wave interaction, where the frequency would decrease as the

magnetic field increases. Thus the oscillation is from the backward wave instability. Initial extracted power from the data shots ranged from 0.1 to 2 MW (± 3 dB).

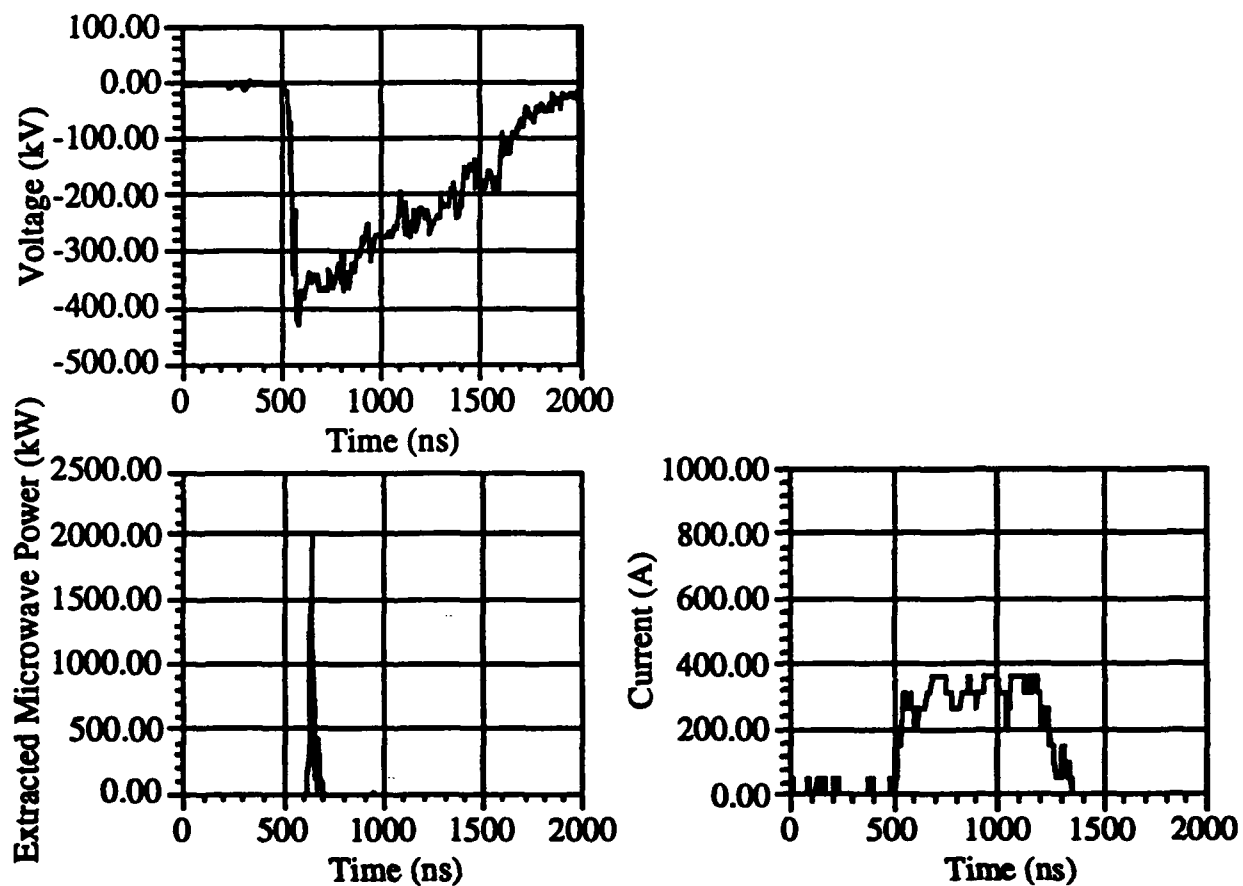


Figure 10. Typical data obtained from the experiment.

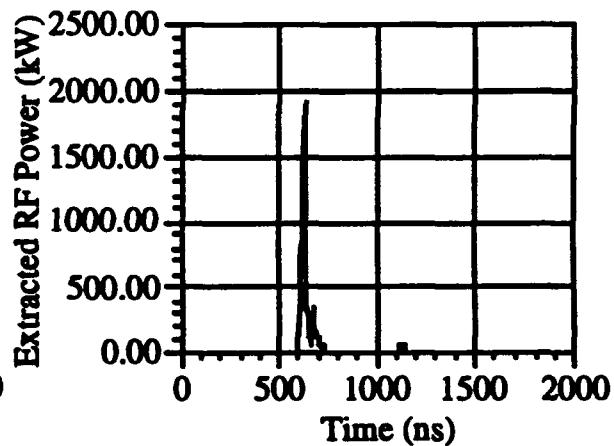
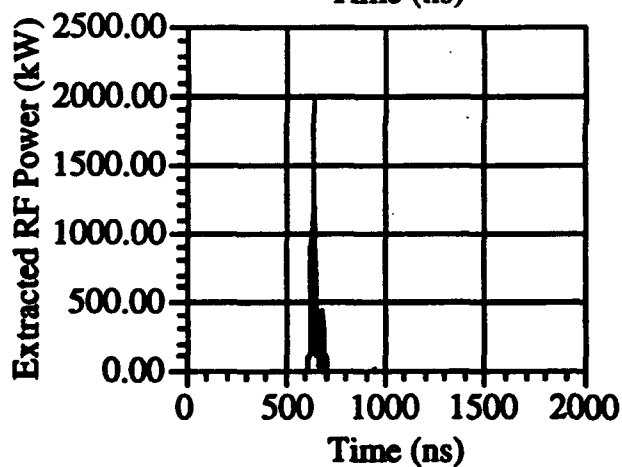
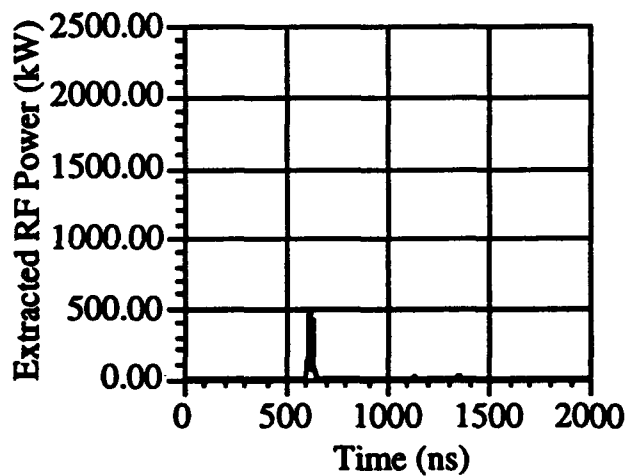


Figure 11. Typical data obtained from the experiment. These data were obtained as part of Figure 10 (that is, the data was obtained on the same shot as Figure 11).

4.0 CONCLUSIONS AND FUTURE WORK

A Gyro-BWO high-power microwave (HPM) device was designed and constructed in FY92 and initial testing of the device was begun. Initial data have shown that the oscillation produced in the device was from that of the Gyro-BWO instability, and that there is magnetic tunability of the frequency. Power extracted (only power that existed in the waveguide detection system was measured; not the actual power of the device itself since a complete calibration of the Vlasov-type antenna has not been done) was shown to be ~ 0.1 to 2 MW (± 3 dB), and that the frequency was able to be chosen between 4.0 to 4.4 GHz by adjusting the magnetic field. Several problems were encountered, one of which being diode closure which limited the pulse length of the RF signal.

Many unanswered questions about the Gyro-BWO still exist. With approximately only 50 to 100 data shots taken for FY92, the Gyro-BWO still needs intensive study and many issues associated with the present device need to be addressed. The first and foremost issue, expected to be completed in FY93, will be to concentrate on lengthening the RF pulse length. This is a must in terms of increasing the amount of energy contained within the RF pulse. Another issue is how much power can be extracted. An additional Vlasov-type C-band antenna will be placed 90 deg. (azimuthally) from the present Vlasov to investigate additional power extraction and perhaps mode identification (also scheduled to be completed in FY93).

Other issues (to be addressed sometime in the future, but not necessarily in FY93) are (1) interband tunability, in terms of how small (or large) a change in the magnetic field before mode 'hopping' (that is, changing from a TE_{01} to a TE_{02} mode) occurs; (2) different power extraction techniques, in terms of reflection type Gyro-BWO designs versus using Vlasov antennas. This may be necessary if frequency tunability is required that goes 'out of band' for a specific waveguide; (3) continue to increase the interaction tube current which is also required in terms of both absolute power and energy available for extraction from the e-beam; (4) intraband tunability to increase the frequencies available for extraction (for perhaps 8 to 10 GHz, or even higher), and how the power availability is affected by moving from one mode to another; and (5) mode stability. That is, how stable is the chosen mode; is there a lot of competition from other modes, what percent of the RF pulse is only such and such a mode, etc.

As can be seen from the above listing, the present Gyro-BWO device has only just begun to be investigated and that there are still many issues to be addressed in future work.

REFERENCES

1. Park, S. Y., Kyser, R. H., Armstrong, C. M., Parker, R. K., and Granatstein, V. L., "Experimental Study of a Ka-Band Gyrotron Backward-Wave Oscillator," I.E.E.E. Trans. Plasma Sci., PS-18 (3), pp. 321-324, June 1990.
2. Spencer, T. A., "High Current, Long-Pulse Gyrotron-Backward-Wave Oscillator Experiments," Ph. D. Dissertation, University of Michigan, Ann Arbor, MI, 1991.
3. Spencer, T. A., Gilgenbach, R. M., and Choi, J. J., "Gyrotron-backward-wave-oscillator experiments utilizing a high current, high voltage, microsecond electron accelerator," J. Appl. Phys. 72 (4), pp. 1221 - 1224, 15 August 1992
4. Guss, W. C., Kriesher, K. E., Temkin, R. J., Caplan, M., and Pirkle, D., "Operation of a 140 GHz Tunable Backward Wave Gyrotron Oscillator," Fourteenth International Conference on Infrared and Millimeter Wave, pp. 369-370, 1989.
5. Baston, M. A., Guss, W. C., Kriesher, K. E., Temkin, R. J., Caplan, M., and Kulke, B., "Operation of a 140 GHz Backward-Wave Oscillator," Fifteenth International Conference on Infrared and Millimeter Wave, pp. 575-577, 1990.
6. Lau, Y. Y., Chu, K. R., Barnett, L. R., and Granatstein, V. L., "Gyrotron Traveling Wave Amplifier: I. Analysis of Oscillations," Inter. J. Infr. and Millimeter Waves, Vol. 2, No. 3, pp. 373-393, 1981.
7. Park, S. Y., Granatstein, V. L., and Parker, R. K., "A Linear Design Study for a Gyrotron Backward-Wave Oscillator," Int. J. Electron., Vol. 57, pp. 1109-1123, 1984.
8. Ganguly, A. K. and Ahn, S., "Optimization of the efficiency in gyrotron backward-wave oscillator via a tapered axial magnetic field," Appl. Phys. Lett. 54 (6), pp. 514-516, 6 February 1989.
9. Gilgenbach, R. M., Walter, M. T., Menge, P. R., and Spencer, T. A., "High Power Gyrotron-Backward-Wave-Oscillator Tapered Interaction Experiments Utilizing Microsecond, Intense E-Beams," The 1992 annual Meeting of the Division of Plasma Physics Conference, November 1992.
10. Hermannsfeldt, W. B., Electron Trajectory Program, SLAC-226, Stanford Linear Accelerator Group, Stanford, CA, 1979.
11. Goplen, B., Ludeking, L., Smithe, D., and Warren, G., The Magic Users Manual, MRC/WDC-R-282, Mission Research Corporation, Alexandria, VA, 1991.

Appendix A

Radiation Hazard Calculations

The following is the Microsoft XL 4.0 (Ref. A.1) spreadsheet used in calculating the Radiation Dose hazard from the RAMBO pulser. The methodology follows that of Kyle Hendricks (Ref. A.2) based on the original setup done in MathCad on an IBM PC compatible. Table A.1 has the actual input and output values. Table A.2 has the input values and the formulas from the XL 4.0 worksheet. The formulas used come from the NRL Plasma Formulary handbook (Ref. A.3).

Table A.1. Input and output values of the radiation dose calculation

RAMBO		
Voltage	0.55	MV
Current	1500	Amps
Pulse_Length	1.00E-06	Seconds
Z	26	(Unitless)
Max_Energy	1.60E+05	Joules
Shots	40	(Unitless)
Radia_Atten due to 24" of Concrete w/ 1/10	1.70E-06	layer thickness of 4.16"
Charge	0.0015	(Coulombs)
Rad Dose @ 1 meter	0.2151	rad/shot
Rad Dose @ 1 meter / Day	8.6049	rad/day
Calc of Total Credible Dose per day @ 2 m (min dis)	3.66E-06	
and per day @ 5 m (max dis)	5.85E-07	

Table A.2. Input and formulas used in the radiation dose calculation.

RAMBO		
Voltage	0.55	MV
Current	1500	Amps
Pulse_Length	0.000001	Seconds
Z	26	(Unitless)
Max_Energy	160000	Joules
Shots	40	(Unitless)
Radia_Atten due to 24" of Concrete w/ 1/10	0.0000017	layer thickness of 4.16"
Charge	=Current*Pulse_Length	(Coulombs)
Rad Dose @ 1 meter	=150*Voltage^2.8*Charge* SQRT(Z)	rad/shot
Rad Dose @ 1 meter / Day	=R[-1]*C* R[-6]*C	rad/day
Calc of Total Credible Dose per day @ 2 m (min dis)	=R[-3]*C* R[-8]*C/2^2	
and per day @ 5 m (max dis)	=R[-4]*C* R[-9]*C/5^2	

REFERENCES

- A.1 Microsoft Excel User's Guide 1 and 2, Document Number XL26296-1092, Microsoft Corp., Redmon, Washington, 1992.
- A.2 Hendricks, Kyle J., Ionizing Radiation Survey, PL-TN--91-1035, Phillips Laboratory, Kirtland AFB, NM, 1991.
- A.3 Book, D. L., NRL Plasma Formulary 1990 Revised Edition, NRL Publication 177-4405, Naval Research Laboratory, Washington, DC, 1990.

Appendix B

Sample Crystal Diode Calibration

The crystal diode detector calibration configuration, shown in Figure B.1, was done as follows. An HP 8350B Sweep Oscillator was used as the frequency generator. A previously calibrated 3-dB Power Divider was used to split the signal between an HP 437B Power Meter and the crystal diode detector (in this case an HP 8470B Crystal Diode Detector). The crystal diode detector generates a millivolt signal based on the milliwatt input, and this signal is sent to a Philips PM2525 Multimeter.

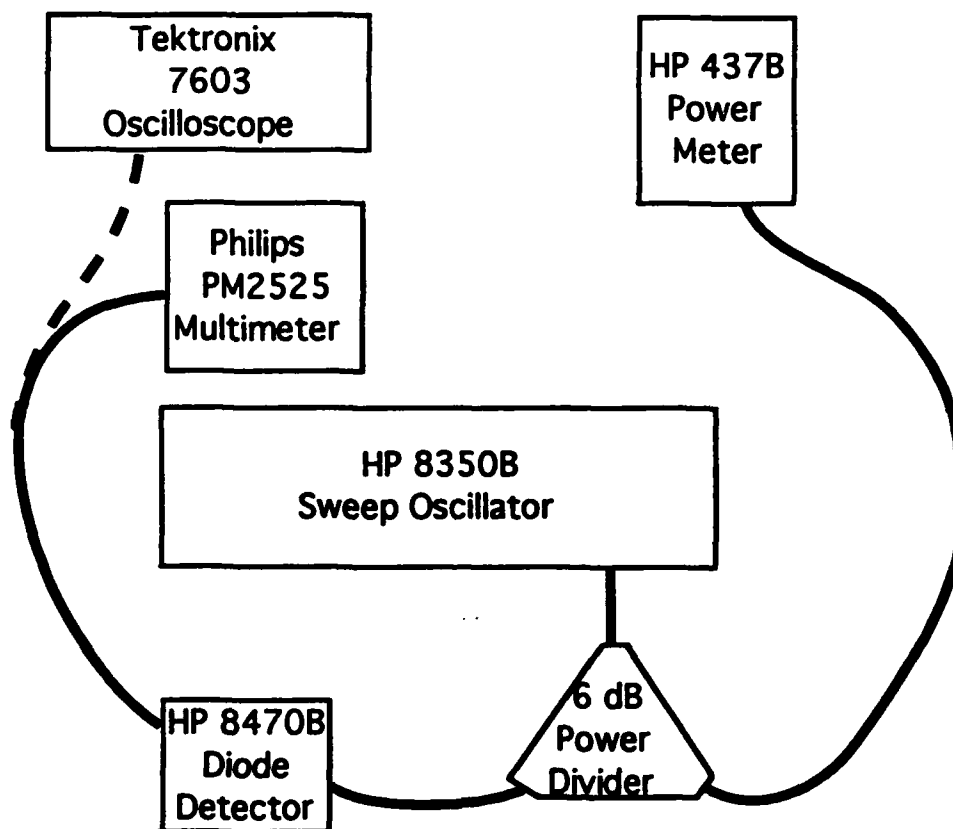


Figure B.1. Experimental configuration used for the crystal diode calibration.

Initially, a frequency range of interest is selected, corresponding to a start and stop frequency on the sweep oscillator, and this signal is displayed on a Tektronix 7603 Oscilloscope to determine the relative flatness of the diode detector signal over this frequency range (4-5 GHz for example). A center frequency (4.5 GHz for the diode data in Table B.1) is then chosen to begin taking data for the diode detector. Table B.1 has an example of data obtained using the above configuration for crystal diode detector #1.

Table B.1. Measured values from crystal diode #1 using the configuration shown in Figure D.1.

mV	dBm
1.32	-12.28
1.50	-11.71
1.99	-10.53
2.59	-9.41
3.29	-8.34
4.15	-7.31
5.20	-6.29
6.45	-5.28
7.91	-4.29
9.65	-3.29
11.74	-2.29
14.17	-1.28
16.97	-0.30
20.15	0.68
23.84	1.67
28.10	2.66
33.04	3.66
38.72	4.66
45.22	5.68
52.66	6.70

Figure B.2 has a plot of the Table B.1 data. A second (or any degree; the ASYST data acquisition system set up by M. Collins Clark [SNLA] uses a fifth) order equation can be fit to the above numbers, which gives an equation that can be used over the frequency spectrum of calibration (in this case, 4 to 5 GHz).

Second Order:

$$P(mW) = 9.52 \times 10^{-4} V^2 + 3.85 \times 10^{-2} V + 8.13 \times 10^{-3} \quad (B.1)$$

Fifth Order:

$$P(mW) = 6.20 \times 10^{-7} V^5 + 9.36 \times 10^{-5} V^4 + 5.32 \times 10^{-3} V^3 + 0.145 V^2 + 2.15 V - 14.40 \quad (B.2)$$

where P is the power in milliwatts and V is the voltage from the crystal in millivolts. These equations are used for determining the RF power in the waveguide detection configuration (see Section 2.0). The fifth-order equation (B.2) is not the same as calculated in the ASYST program. The ASYST program calculates the fifth-order

equation in terms of watts and volts for the power and voltage. Equations B.1 and B.2 were produced by DeltaGraph Pro for the Macintosh.

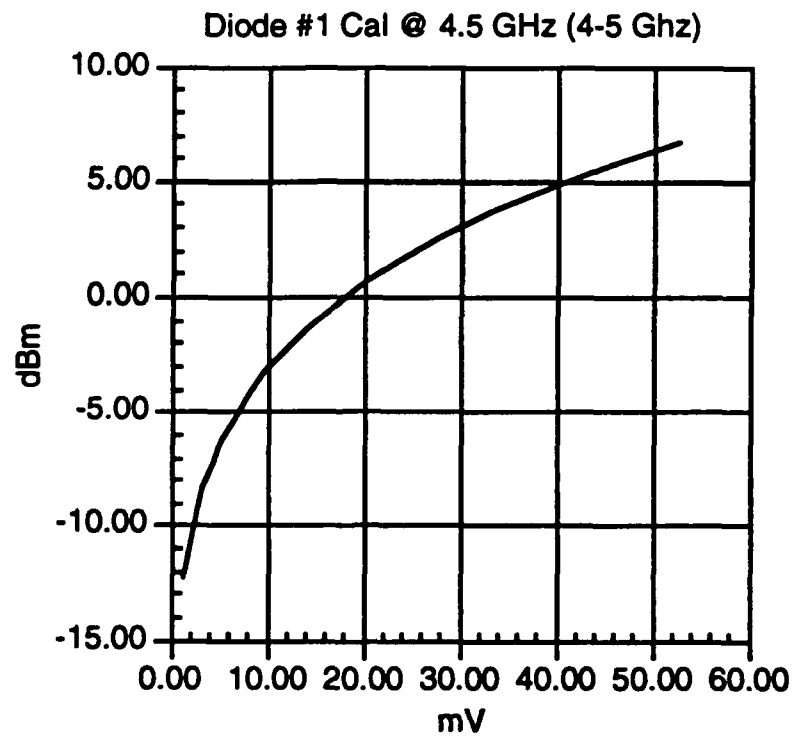


Figure B.2. Plot of the Table B.1 data for the crystal diode #1.

Appendix C

Sample Cable Calibration

The cable calibration configuration is shown in Figure C.1. This calibration is used to find the attenuation of the data cables for a given frequency sweep. The cables are those that run from the experiment to the screen room and any others that need to be calibrated. Since the cables are 30 to 45 m, the attenuation factor can be rather large (20 to 30 dB). An HP 8757A (or D) is used for the cable calibrations. The HP 85025A detector and its attached cable are 'zeroed out' by connecting to the HP 85027C Directional Bridge and taking a frequency sweep measurement. A frequency range of interest is specified and then a frequency sweep measurement is taken. This is used as a zero reference point. Next, a cable that needs to be calibrated is connected between the detector and directional bridge, and a measurement is taken. Figure C.2 has an example of a frequency sweep plot. From the plot, one gets a calibration curve (a linear equation in most cases) that is used for determining the attenuation at a given frequency for the cable.

The equation for Figure C.2. would be (linear fit in this case),

$$dB = 5.841(Frequency) + 5.134 \quad (C.1)$$

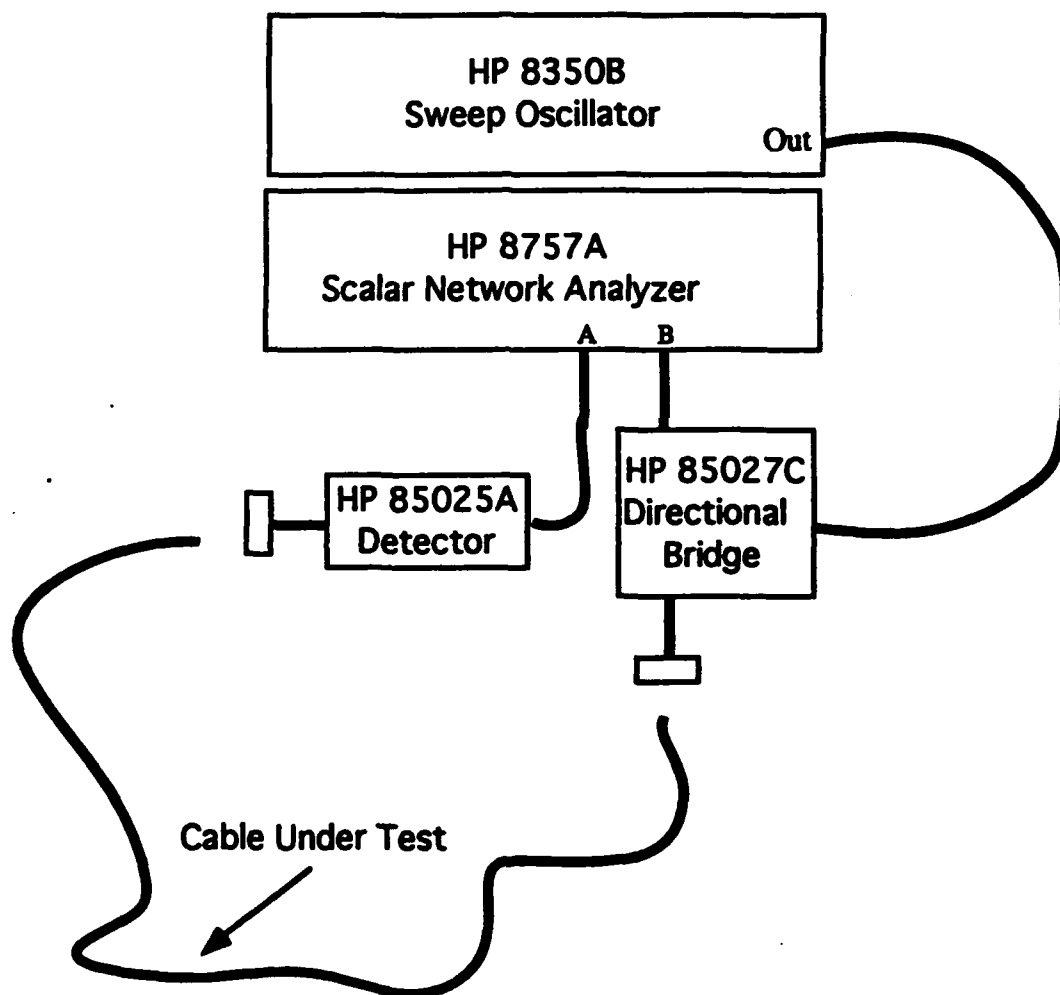


Figure C.1. Cable calibration configuration.

CH2: B -M A - 48.26 dB
 5.0 dB/ REF - 15.00 dB

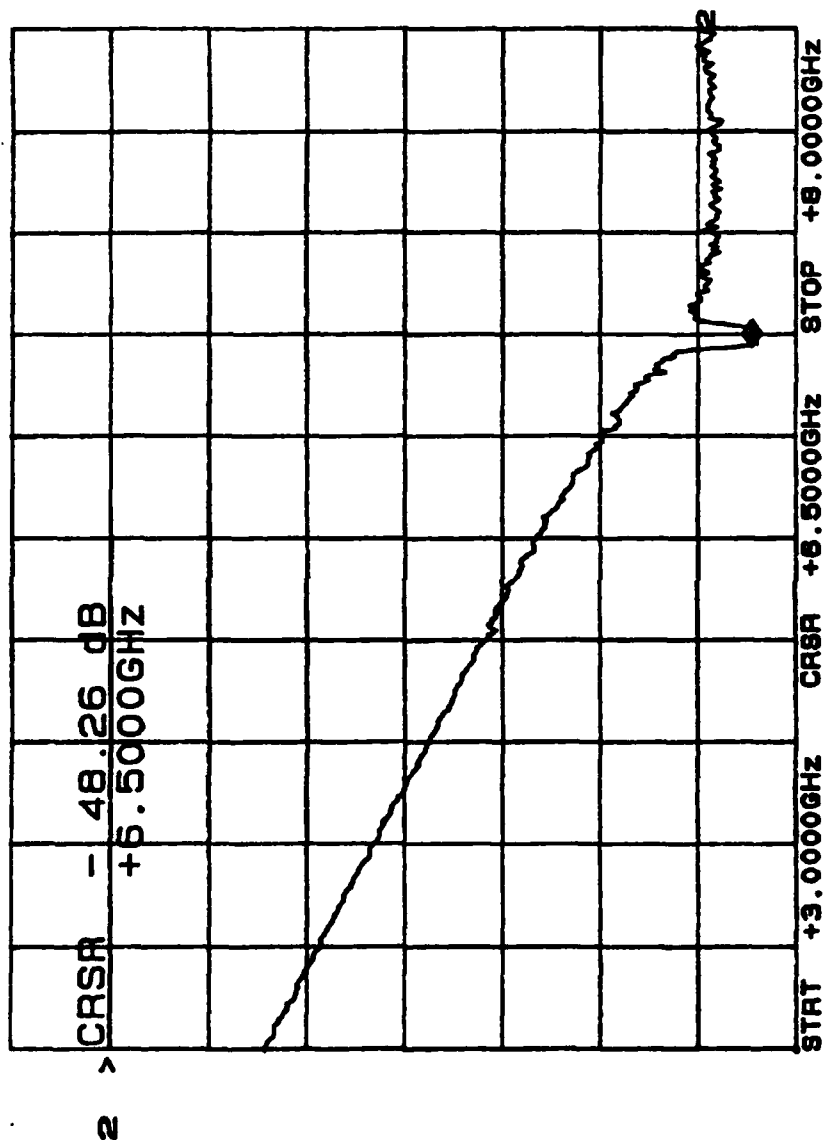


Figure C.2. Cable calibration curve obtained from the HP 8757A Scalar Network Analyzer.

Appendix D

ASYST Channel Setups

The following contains the ASYST scope channel setups and the ASYST generated crystal diode equations (see Appendix B for further information on crystal diode calibrations).

Channel #: 5 Hp54111D C:CH5.S8
TYPE: HP54111D
STATUS: ON
TITLE: MARX VOLTAGE
ADDRESS: B:0 G:1 CH:1
ATTN (dB): FIXED: 88.58 CABLE: .00 OTHER: .00
INTEG(RC):
CABLE #: 46 1-WAY DELAY(SEC): 2.791E-7 08/31/92
PROBE #: 0 NOT CONFIGURED SEN: 1. VOLTS
POSITION:
DETECTOR : NONE
COMMENT: RAMBO MARX VOLTAGE 1528 V/V 2X 2X 10X ATTN
VOLTS/DIV: 5V/DIV
COUPLING: AC
OFFSET(DIV): 2
SWEEP SPEED: 500ns/div (10 ns/div)
SWEEP DELAY: DELAY-3 REFERENCE: CENT
TRIG SETUP: DCFIFTY EXT-3/10 POS
TRIG LEVEL: .300
DATA INCREMENT: 1X

Channel #: 6 Hp54111D C:CH6.S8
TYPE: HP54111D
STATUS: ON
TITLE: MARX CURRENT
ADDRESS: B:0 G:1 CH:2
ATTN (dB): FIXED: .00 CABLE: .00 OTHER: .00
INTEG(RC): 1.53E2 uSEC
CABLE #: 47 1-WAY DELAY(SEC): 2.691E-7 08/31/92
PROBE #: 0 NOT CONFIGURED SEN: 1. VOLTS
POSITION:
DETECTOR : NONE
COMMENT: RAMBO CURRENT
VOLTS/DIV: 100mV/DIV
COUPLING: AC
OFFSET(DIV): 0
SWEEP SPEED: LOCAL
SWEEP DELAY: LOCAL REFERENCE: LEFT
TRIG SETUP: DCFIFTY EXT-3 POS
TRIG LEVEL: .300
DATA INCREMENT: 1X

Channel #: 7 Hp54111D C:CH7.S8
TYPE: HP54111D
STATUS: ON
TITLE: MAGNIFORM CURRENT
ADDRESS: B:0 G:2 CH:1
ATTN (dB): FIXED: .00 CABLE: .00 OTHER: .00
INTEG(RC):
CABLE #: 45 1-WAY DELAY(SEC): 2.439E-7 08/31/92
PROBE #: 0 NOT CONFIGURED SEN: 1. VOLTS
POSITION:
DETECTOR : NONE
COMMENT:
VOLTS/DIV: 5V/DIV

COUPLING: AC
OFFSET(DIV): 2
SWEEP SPEED: 5ms/div (10 ns/div)
SWEEP DELAY: DELAY-7 REFERENCE: CENT
TRIG SETUP: DC EXT-3 POS
TRIG LEVEL: .300
DATA INCREMENT: 1X

Channel #: 9 Hp54111D C:CH9.S8
TYPE: HP54111D
STATUS: ON
TITLE: UPSTREAM ROGOWSKI
ADDRESS: B:0 G:3 CH:1
ATTN (dB): FIXED: .00 CABLE: .00 OTHER: .00
INTEG(RC): 2.56E1 uSEC
CABLE #: 50 1-WAY DELAY(SEC): 2.408E-7 08/31/92
PROBE #: 0 NOT CONFIGURED SEN: 1. VOLTS
POSITION:
DETECTOR : NONE
COMMENT: UPSTREAM ROGOWSKI 79.9 A/MV
VOLTS/DIV: 20mV/DIV
COUPLING: AC
OFFSET(DIV): -1
SWEEP SPEED: 200ns/div (4ns/div)
SWEEP DELAY: DELAY-7 REFERENCE: CENT
TRIG SETUP: DC EXT-3 POS
TRIG LEVEL: .300
DATA INCREMENT: 1X

Channel #: 10 Hp54111D C:CH10.S8
TYPE: HP54111D
STATUS: ON
TITLE: DOWNSTREAM ROGOWSKI
ADDRESS: B:0 G:3 CH:2
ATTN (dB): FIXED: .00 CABLE: .00 OTHER: .00
INTEG(RC): 2.56E1 uSEC
CABLE #: 51 1-WAY DELAY(SEC): 2.428E-7 08/31/92
PROBE #: 0 NOT CONFIGURED SEN: 1. VOLTS
POSITION:
DETECTOR : NONE
COMMENT: DOWNSTREAM ROGOWSKI 83.5 A/MV
VOLTS/DIV: 20mV/DIV
COUPLING: AC
OFFSET(DIV): -1
SWEEP SPEED: 200ns/div (4ns/div)
SWEEP DELAY: LOCAL REFERENCE: LEFT
TRIG SETUP: DC EXT-3 POS
TRIG LEVEL: .300
DATA INCREMENT: 1X

Channel #: 11 Hp54111D C:CH11.S8
TYPE: HP54111D
STATUS: OFF
TITLE: WAVEGUIDE DIAG #2
ADDRESS: B:0 G:4 CH:1
ATTN (dB): FIXED: 53.00 CABLE: .00 OTHER: .00
INTEG(RC):
CABLE #: 53 1-WAY DELAY(SEC): 2.449E-7 08/31/92
PROBE #: 0 NOT CONFIGURED SEN: 1. VOLTS
POSITION:
DETECTOR : uW-XTAL: 1 HP 8470B #5
COMMENT: WAVEGUIDE DIAG, 50 dB GUIDE ATTEN
VOLTS/DIV: 10mV/DIV
COUPLING: AC

OFFSET(DIV): 3
SWEEP SPEED: 200ns/div (4ns/div)
SWEEP DELAY: DELAY-7 REFERENCE: LEFT
TRIG SETUP: DC EXT-3 POS
TRIG LEVEL: .300
DATA INCREMENT: 1X

Channel #: 12 Hp54111D C:CH12.S8
TYPE: HP54111D
STATUS: OFF
TITLE: WAVEGUIDE DIAG #1
ADDRESS: B:0 G:4 CH:2
ATTN (dB): FIXED: 48.00 CABLE: .00 OTHER: .00
INTEG(RC):
CABLE #: 52 1-WAY DELAY(SEC): 2.446E-7 08/31/92
PROBE #: 0 NOT CONFIGURED SEN: 1. VOLTS
POSITION:
DETECTOR : uW-XTAL: 2 HP 8470B #6
COMMENT: WAVEGUIDE DIAG #1, 30 dB GUIDE ATTEN
VOLTS/DIV: 20mV/DIV
COUPLING: AC
OFFSET(DIV): 2
SWEEP SPEED: LOCAL
SWEEP DELAY: LOCAL REFERENCE: LEFT
TRIG SETUP: DC EXT-3 POS
TRIG LEVEL: .300
DATA INCREMENT: 1X

Channel #: 13 Hp54111D C:CH13.S8
TYPE: HP54111D
STATUS: ON
TITLE: LARGE ROGOWSKI
ADDRESS: B:0 G:6 CH:1
ATTN (dB): FIXED: .00 CABLE: .00 OTHER: .00
INTEG(RC): 2.101E1 uSEC
CABLE #: 49 1-WAY DELAY(SEC): 2.760E-7 08/31/92
PROBE #: 0 NOT CONFIGURED SEN: 1. VOLTS
POSITION:
DETECTOR : NONE
COMMENT: 6.56E9 A/(V-S)
VOLTS/DIV: 20mV/DIV
COUPLING: AC
OFFSET(DIV): 0
SWEEP SPEED: 200ns/div (4ns/div)
SWEEP DELAY: DELAY-7 REFERENCE: LEFT
TRIG SETUP: DC EXT-3 POS
TRIG LEVEL: .300
DATA INCREMENT: 1X

Channel #: 14 Hp54111D C:CH13.S8
TYPE: HP54111D
STATUS: ON
TITLE: SGHORN AT OUTPUT WINDOW
ADDRESS: B:0 G:6 CH:2
ATTN (dB): FIXED: 40.00 CABLE: 25.00 OTHER: .00
INTEG(RC):
CABLE #: 54 1-WAY DELAY(SEC): 2.458E-7 08/31/92
PROBE #: 0 NOT CONFIGURED SEN: 1. VOLTS
POSITION:
DETECTOR : uW-XTAL: 3 HP 8470B #4
COMMENT:
VOLTS/DIV: 5mV/DIV
COUPLING: AC

OFFSET(DIV): 3
SWEEP SPEED: LOCAL
SWEEP DELAY: LOCAL REFERENCE: CENT
TRIG SETUP: DC EXT-3 POS
TRIG LEVEL: .300
DATA INCREMENT: 1X

Channel #: 81 Hp16500A C:CH81.S8
TYPE: HP16500A
STATUS: ON
TITLE: WAVEGUIDE DIAG #2
ADDRESS: B:0 G:5 CH:1
ATTN (dB): FIXED: 50.00 CABLE: 24.00 OTHER: 12.00
INTEG(RC): 0 uSEC
CABLE #: 53 1-WAY DELAY(SEC): 2.449E-7 08/31/92
PROBE #: 0 NOT CONFIGURED SEN: 1. VOLTS
POSITION:
DETECTOR : uW-XTAL: 1 HP 8470B #5
COMMENT: WAVEGUIDE #2 50.0 dB GUIDE ATTEN.
VOLTS/DIV: 20mV/DIV
COUPLING: DC
OFFSET(DIV): 2
SWEEP SPEED: 200ns/div (4ns/div)
SWEEP DELAY: DELAY-7 REFERENCE: CENT
TRIG SETUP: DCFIFITY EXT-3 POS
TRIG LEVEL: 3.00E-1
DATA INCREMENT: 2X

Channel #: 82 Hp16500A C:CH82.S8
TYPE: HP16500A
STATUS: ON
TITLE: WAVEGUIDE DIAG #1
ADDRESS: B:0 G:5 CH:2
ATTN (dB): FIXED: 30.00 CABLE: 24.00 OTHER: 35.00
INTEG(RC):
CABLE #: 52 1-WAY DELAY(SEC): 2.446E-7 08/31/92
PROBE #: 0 NOT CONFIGURED SEN: 1. VOLTS
POSITION:
DETECTOR : uW-XTAL: 2 HP 8470B #6
COMMENT: WAVEGUIDE #1 30.0 dB GUIDE ATTEN.
VOLTS/DIV: 20mV/DIV
COUPLING: DC
OFFSET(DIV): 2
SWEEP SPEED: LOCAL
SWEEP DELAY: LOCAL REFERENCE: LEFT
TRIG SETUP: DCFIFITY EXT-3 POS
TRIG LEVEL: 0.3
DATA INCREMENT: 2X

Channel #: 83 Hp16500A C:CH83.S8
TYPE: HP16500A
STATUS: ON
TITLE: HETERODYNE SIGNAL
ADDRESS: B:0 G:5 CH:3
ATTN (dB): FIXED: .00 CABLE: .00 OTHER: .00
INTEG(RC):
CABLE #: 53 1-WAY DELAY(SEC): 2.449E-7 08/31/92
PROBE #: 0 NOT CONFIGURED SEN: 1. VOLTS
POSITION:
DETECTOR : NONE
COMMENT: 4.8 GHz LO SIGNAL
VOLTS/DIV: 40mV/DIV
COUPLING: DC

OFFSET(DIV): 0
SWEEP SPEED: LOCAL
SWEEP DELAY: LOCAL REFERENCE: LEFT
TRIG SETUP: DCFIFITY EXT-3 POS
TRIG LEVEL: 0.30
DATA INCREMENT: 2X

Channel #: 84 Hp16500A C:CH84.S8
TYPE: HP16500A
STATUS: ON
TITLE: STANDARD GAIN HORN (DOWNSTREAM)
ADDRESS: B:0 G:5 CH:4
ATTN (dB): FIXED: 40.00 CABLE: 25.00 OTHER: .00
INTEG(RC):
CABLE #: 54 1-WAY DELAY(SEC): 2.458E-7 08/31/92
PROBE #: 0 NOT CONFIGURED SEN: 1. VOLTS
POSITION:
DETECTOR : uW-X TAL: 3 HP 8470B #4
COMMENT: STANDARD GAIN HORN SIGNAL DOWNSTREAM OUTPUT
VOLTS/DIV: 10mV/DIV
COUPLING: DC
OFFSET(DIV): 2
SWEEP SPEED: LOCAL
SWEEP DELAY: LOCAL REFERENCE: LEFT
TRIG SETUP: DCFIFITY EXT-3 POS
TRIG LEVEL: 0.30
DATA INCREMENT: 2X

Channel #: 85 Hp16500A C:CH85.S8
TYPE: HP16500A
STATUS: ON
TITLE: 2.6 - 3.95 GHz
ADDRESS: B:0 G:5 CH:5
ATTN (dB): FIXED: 30.00 CABLE: 24.00 OTHER: 35.00
INTEG(RC): 0 uSEC
CABLE #: 52 1-WAY DELAY(SEC): 2.446E-7 08/31/92
PROBE #: 0 NOT CONFIGURED SEN: 1. VOLTS
POSITION:
DETECTOR : uW-X TAL: 4 HP 8470B #3
COMMENT: 2.6 - 3.95 GHz BPF OFF WAVEGUIDE DIAG #1
VOLTS/DIV: 10mV/DIV
COUPLING: DC
OFFSET(DIV): 2
SWEEP SPEED: LOCAL
SWEEP DELAY: LOCAL REFERENCE: LEFT
TRIG SETUP: DCFIFITY EXT-3 POS
TRIG LEVEL: 0.30
DATA INCREMENT: 2X

ASYST crystal cals:

#1: HP 8470B #5

Polynomial Coef. A0-A5

1.9919e3 -2.4111e2 1.0077e1 7.6436e-1 3.7576e-2 5.1463e-6

#2: HP 8470B #6

Polynomial Coef. A0-A5

-2.5143e3 2.5800e2 -9.5395e0 1.0895e0 3.7140e-2 3.3355e-6

#3: HP 8470B #4

Polynomial Coef. A0-A5

2.8436e3 -3.5846e2 1.5490e1 6.4677e-1 3.8986e-2 3.3740e-6

#4: HP 8470B #3

Polynomial Coef. A0-A5

1.7370e3 -2.4605e2 1.2305e1 6.8154e-1 3.9858e-2 6.9268e-6

Appendix E

Sample Magnet Input Data Deck For the Gyro-BWO

This is a sample input deck for the Gyro-BWO Magnet setup (both the DC Coils and Helmholtz pair).

The first line lists the total number of coils, 'n', to be input into the simulation. The second through 'n'+1 lines give the actual data input for the coils. The first number is the radius location of the first coil, the second and third numbers give the width of the coil, the fourth number gives the number of coils at that position (in case you wish to only use one input line at an average radius with x number of coils), and the fifth number is the current to be put into the coils (usually set to an Amp for a gauss per Ampere output). Note that the following are in centimeters.

```

287
2.219325E+01 8.340000E+01 9.102000E+01 1 1.000000E+00
2.225675E+01 8.340000E+01 9.102000E+01 1 1.000000E+00
2.232025E+01 8.340000E+01 9.102000E+01 1 1.000000E+00
2.238375E+01 8.340000E+01 9.102000E+01 1 1.000000E+00
2.244726E+01 8.340000E+01 9.102000E+01 1 1.000000E+00
2.251076E+01 8.340000E+01 9.102000E+01 1 1.000000E+00
2.257426E+01 8.340000E+01 9.102000E+01 1 1.000000E+00
2.263776E+01 8.340000E+01 9.102000E+01 1 1.000000E+00
2.270126E+01 8.340000E+01 9.102000E+01 1 1.000000E+00
2.276476E+01 8.340000E+01 9.102000E+01 1 1.000000E+00
2.282826E+01 8.340000E+01 9.102000E+01 1 1.000000E+00
2.289177E+01 8.340000E+01 9.102000E+01 1 1.000000E+00
2.295527E+01 8.340000E+01 9.102000E+01 1 1.000000E+00
2.301877E+01 8.340000E+01 9.102000E+01 1 1.000000E+00
2.308227E+01 8.340000E+01 9.102000E+01 1 1.000000E+00
2.314577E+01 8.340000E+01 9.102000E+01 1 1.000000E+00
2.320927E+01 8.340000E+01 9.102000E+01 1 1.000000E+00
2.327277E+01 8.340000E+01 9.102000E+01 1 1.000000E+00
2.333628E+01 8.340000E+01 9.102000E+01 1 1.000000E+00
2.339978E+01 8.340000E+01 9.102000E+01 1 1.000000E+00
2.346328E+01 8.340000E+01 9.102000E+01 1 1.000000E+00
2.352678E+01 8.340000E+01 9.102000E+01 1 1.000000E+00
2.359028E+01 8.340000E+01 9.102000E+01 1 1.000000E+00
2.365378E+01 8.340000E+01 9.102000E+01 1 1.000000E+00
2.371728E+01 8.340000E+01 9.102000E+01 1 1.000000E+00
2.378078E+01 8.340000E+01 9.102000E+01 1 1.000000E+00
2.384429E+01 8.340000E+01 9.102000E+01 1 1.000000E+00
2.390779E+01 8.340000E+01 9.102000E+01 1 1.000000E+00
2.397129E+01 8.340000E+01 9.102000E+01 1 1.000000E+00
2.403479E+01 8.340000E+01 9.102000E+01 1 1.000000E+00
2.409829E+01 8.340000E+01 9.102000E+01 1 1.000000E+00
2.416179E+01 8.340000E+01 9.102000E+01 1 1.000000E+00
2.422529E+01 8.340000E+01 9.102000E+01 1 1.000000E+00
2.428880E+01 8.340000E+01 9.102000E+01 1 1.000000E+00
2.435230E+01 8.340000E+01 9.102000E+01 1 1.000000E+00
2.441580E+01 8.340000E+01 9.102000E+01 1 1.000000E+00
2.447930E+01 8.340000E+01 9.102000E+01 1 1.000000E+00
2.454280E+01 8.340000E+01 9.102000E+01 1 1.000000E+00
2.460630E+01 8.340000E+01 9.102000E+01 1 1.000000E+00
2.466980E+01 8.340000E+01 9.102000E+01 1 1.000000E+00
2.473330E+01 8.340000E+01 9.102000E+01 1 1.000000E+00
2.479681E+01 8.340000E+01 9.102000E+01 1 1.000000E+00
2.486031E+01 8.340000E+01 9.102000E+01 1 1.000000E+00
2.492381E+01 8.340000E+01 9.102000E+01 1 1.000000E+00

```

33

34

35

2.625734E+01	1.269000E+02	1.345200E+02	1	1.000000E+00
2.632084E+01	1.269000E+02	1.345200E+02	1	1.000000E+00
2.638434E+01	1.269000E+02	1.345200E+02	1	1.000000E+00
2.644784E+01	1.269000E+02	1.345200E+02	1	1.000000E+00
2.651134E+01	1.269000E+02	1.345200E+02	1	1.000000E+00
2.657484E+01	1.269000E+02	1.345200E+02	1	1.000000E+00
2.663835E+01	1.269000E+02	1.345200E+02	1	1.000000E+00
2.670185E+01	1.269000E+02	1.345200E+02	1	1.000000E+00
2.676535E+01	1.269000E+02	1.345200E+02	1	1.000000E+00
2.682885E+01	1.269000E+02	1.345200E+02	1	1.000000E+00
2.689235E+01	1.269000E+02	1.345200E+02	1	1.000000E+00
2.695585E+01	1.269000E+02	1.345200E+02	1	1.000000E+00
2.701935E+01	1.269000E+02	1.345200E+02	1	1.000000E+00
2.708286E+01	1.269000E+02	1.345200E+02	1	1.000000E+00
2.714636E+01	1.269000E+02	1.345200E+02	1	1.000000E+00
2.720986E+01	1.269000E+02	1.345200E+02	1	1.000000E+00
2.727336E+01	1.269000E+02	1.345200E+02	1	1.000000E+00
2.733686E+01	1.269000E+02	1.345200E+02	1	1.000000E+00
2.740036E+01	1.269000E+02	1.345200E+02	1	1.000000E+00
2.746386E+01	1.269000E+02	1.345200E+02	1	1.000000E+00
2.752736E+01	1.269000E+02	1.345200E+02	1	1.000000E+00
2.759087E+01	1.269000E+02	1.345200E+02	1	1.000000E+00
2.765437E+01	1.269000E+02	1.345200E+02	1	1.000000E+00
2.771787E+01	1.269000E+02	1.345200E+02	1	1.000000E+00
2.778137E+01	1.269000E+02	1.345200E+02	1	1.000000E+00
2.784487E+01	1.269000E+02	1.345200E+02	1	1.000000E+00
2.790837E+01	1.269000E+02	1.345200E+02	1	1.000000E+00
2.797187E+01	1.269000E+02	1.345200E+02	1	1.000000E+00
2.803538E+01	1.269000E+02	1.345200E+02	1	1.000000E+00
2.809888E+01	1.269000E+02	1.345200E+02	1	1.000000E+00
2.816238E+01	1.269000E+02	1.345200E+02	1	1.000000E+00
2.822588E+01	1.269000E+02	1.345200E+02	1	1.000000E+00
2.828938E+01	1.269000E+02	1.345200E+02	1	1.000000E+00
2.835288E+01	1.269000E+02	1.345200E+02	1	1.000000E+00
2.841638E+01	1.269000E+02	1.345200E+02	1	1.000000E+00
2.847989E+01	1.269000E+02	1.345200E+02	1	1.000000E+00
2.854339E+01	1.269000E+02	1.345200E+02	1	1.000000E+00
2.860689E+01	1.269000E+02	1.345200E+02	1	1.000000E+00
2.867039E+01	1.269000E+02	1.345200E+02	1	1.000000E+00
2.873389E+01	1.269000E+02	1.345200E+02	1	1.000000E+00
2.879739E+01	1.269000E+02	1.345200E+02	1	1.000000E+00
2.886089E+01	1.269000E+02	1.345200E+02	1	1.000000E+00
2.892439E+01	1.269000E+02	1.345200E+02	1	1.000000E+00
2.898790E+01	1.269000E+02	1.345200E+02	1	1.000000E+00
2.905140E+01	1.269000E+02	1.345200E+02	1	1.000000E+00
2.911490E+01	1.269000E+02	1.345200E+02	1	1.000000E+00
2.917840E+01	1.269000E+02	1.345200E+02	1	1.000000E+00
2.924190E+01	1.269000E+02	1.345200E+02	1	1.000000E+00
2.930540E+01	1.269000E+02	1.345200E+02	1	1.000000E+00
2.936890E+01	1.269000E+02	1.345200E+02	1	1.000000E+00
2.943241E+01	1.269000E+02	1.345200E+02	1	1.000000E+00

Appendix F

Sample EGUN Input Data Deck For the Gyro-BWO

This is a sample input deck for the Gyro-BWO diode setup (using both the DC Coils and Helmholtz pair magnet data input from measured data).

Gyro-BWO Set Up w/ RAMBO 7/2/92 Tom Spencer B = 1.5 - 5.00 kG E = 550 kV
 RLIM ZLIM POTN POT(POTN) LSTPOT MI MAGSEG
 31 240 4 0.0,5.5E05,5.5E05,0.0 2 3 -1

1474.122
 1481.393
 1488.778
 1496.283
 1503.912
 1511.671
 1519.564
 1527.598
 1535.776
 1544.104
 1552.589
 1561.234
 1570.045
 1579.027
 1588.187
 1597.529
 1607.058
 1616.78
 1626.701
 1636.825
 1647.157
 1657.704
 1668.471
 1679.462
 1690.682
 1702.137
 1713.832
 1725.771
 1737.961
 1750.404
 1763.106
 1776.072
 1789.306
 1802.812
 1816.595
 1830.659
 1845.007
 1859.644
 1874.573
 1889.797
 1905.32
 1921.144
 1937.274
 1953.711
 1970.457
 1987.51
 2004.58
 2022.578
 2040.584
 2058.588
 2077.552
 2096.516
 2115.8

2135.405
2155.329
2175.573
2196.135
2217.014
2238.209
2259.716
2281.534
2303.66
2326.09
2348.82
2371.846
2395.164
2418.769
2442.654
2466.813
2491.241
2515.929
2540.871
2566.058
2591.482
2617.132
2643.001
2669.076
2695.348
2721.806
2748.436
2775.227
2802.167
2829.24
2856.434
2883.733
2911.123
2938.588
2966.112
2993.678
3021.269
3048.868
3076.458
3104.018
3131.532
3158.98
3186.342
3213.599
3240.732
3267.719
3294.542
3321.178
3347.609
3373.813
3399.771
3425.461
3450.864
3475.958
3500.725
3525.145
3549.198
3572.865
3596.128
3618.969
3641.37
3663.314
3684.785
3705.769

3726.249
3746.212
3765.645
3784.536
3802.874
3820.648
3837.849
3854.47
3870.503
3885.943
3900.784
3915.024
3928.66
3941.69
3954.116
3965.938
3977.159
3987.782
3997.812
4007.256
4016.121
4024.415
4032.146
4039.327
4045.968
4052.082
4057.682
4062.782
4067.397
4071.544
4075.238
4078.497
4081.339
4083.781
4085.844
4087.545
4088.904
4089.941
4090.676
4091.128
4091.318
4091.266
4090.992
4090.515
4089.855
4089.031
4088.063
4086.968
4085.765
4084.471
4083.103
4081.678
4080.212
4078.719
4077.213
4075.708
4074.217
4072.75
4071.321
4069.936
4068.607
4067.34
4066.143
4065.021

4063.98
4063.023
4062.152
4061.37
4060.676
4060.071
4059.553
4059.118
4058.764
4058.485
4058.276
4058.129
4058.036
4057.99
4057.978
4057.992
4058.019
4058.046
4058.06
4058.046
4057.99
4057.876
4057.686
4057.405
4057.013
4056.494
4055.827
4054.994
4053.976
4052.753
4051.303
4049.608
4047.647
4045.4
4042.845
4039.963
4036.734
4033.137
4029.153
4024.763
4019.949
4014.69
4008.971
4002.774
3996.082
3988.879
3981.151
3972.884
3964.064
3954.679
3944.719
3934.172
3923.03
3911.285
3898.93
3885.96
3872.369
3858.154
3843.314
3827.847
3811.754
3795.036
3777.696
3759.737

3741.165
 3721.986
 3702.207
 3681.836
 3660.883
 3639.357
 3617.272
 3594.638

4	0	9	0.0	-0.99
4	4	9	2.0	-0.99
4	7	9	2.0	-0.99
4	8	9	0.99	-0.99
4	8	15	0.99	2.00
4	8	26	0.99	2.00
4	8	27	0.99	2.00
1	9	28	2.0	-0.99
4	10	28	2.0	-0.99
4	11	27	-0.95	2.00
4	11	26	-0.95	2.00
4	11	15	-0.95	2.00
4	11	6	-0.95	2.00
4	10	5	2.00	0.95
4	9	5	2.00	0.95
4	8	5	2.00	0.95
4	7	5	2.00	0.95
4	6	5	2.00	0.95
4	5	5	-0.99	0.95
4	5	4	-0.99	2.0
4	5	3	-0.99	2.0
4	5	2	-0.99	2.0
4	5	1	-0.99	2.0
4	5	0	-0.99	0.0
4	6	0	2.0	0.0
0	28	0	2.0	0.0
0	29	0	2.0	0.0
2	30	0	0.01	0.0
2	30	30	0.01	2.0
2	30	34	0.01	2.0
2	30	35	0.01	0.99
2	29	35	2.0	0.99
2	25	35	2.0	0.99
2	20	35	2.0	0.99
2	19	36	0.6	2.0
2	19	50	0.6	2.0
2	19	211	0.6	2.0
2	19	212	0.6	0.01
2	18	212	2.0	0.01
2	17	212	2.0	0.01
2	16	213	0.072	2.0
2	16	214	0.072	2.0
2	16	216	0.072	2.0
2	16	239	0.072	2.0
2	16	240	0.072	0.0
0	15	240	2.0	0.0
0	4	240	2.0	0.0
0	0	240	0.0	0.0
0	0	100	0.0	2.0
0	0	37	0.0	2.0
3	0	36	0.0	-0.01
3	1	36	2.0	-0.01
3	10	36	2.0	-0.01
3	18	36	2.0	-0.01
3	18	35	2.0	0.99
3	10	35	2.0	0.99

3	1	35	2.0	0.99					
3	0	35	0.0	0.99					
0	0	34	0.0	2.0					
0	0	25	0.0	2.0					
0	0	10	0.0	2.0					

888

UNIT	MAXRAY	STEP	NS	SPC	MASS	ZEND	VION	SAVE	
0.0025	15	0.15	5	0.5	0.0	240	-1.E8		0
START	AV	AVR	RC	ZC	DENS	SURFACE	MAGMLT	MAGORD	
'GENERAL'	0	1.0	8.99	29.01	5000.0	1	1.0		2